



INSTITUTE OF THEORETICAL  
AND EXPERIMENTAL PHYSICS

ITEP - 25

SI 78 024 22

O.D.Dalkarov, B.O.Kerbikov, V.E.Markushin

Acc

ANNIHILATION OF ANTIPROTONS STOPPED IN  
LIQUID HYDROGEN AND DEUTERIUM

M O S C O W 1 9 7 6

O.D.Dalkarov, B.O.Kerbikov, V.E.Markushin

ANNIHILATION OF ANTIPROTONS STOPPED IN  
LIQUID HYDROGEN AND DEUTERIUM

Moscow 1976

A b s t r a c t

Detailed analysis is given of stopping antiproton annihilation in liquid hydrogen and deuterium. Connection between capture schedule and properties of bound states in nucleon-antinucleon system is established. The theoretical predictions are compared with experimental data which appeared in 1971-75.

## Contents

I. Introduction .....	5
II. De-excitation processes.....	6
III. Widths of the atomic levels and annihilation rates .....	7
3.1. Atomic widths .....	8
3.2. Stark mixing .....	14
3.3. Effective annihilation rates .....	22
IV. Cascade calculations .....	24
4.1. The S and P state capture sequence.....	25
4.2. The dependence on the widths of quasi-nuclear states .....	27
4.3. The dependence on the radius of quasi-nuclear P-state .....	28
4.4. The dependence on the energy displacement of the atomic S level .....	28
4.5. The role of the velocity of $\bar{p}$ atom .....	29
4.6. The dependence on the reduced mass of $\bar{p}$ atom .....	29
4.7. I-spin analysis .....	29
4.8. Spin analysis .....	30
4.9. P capture from S orbitals in $\bar{p}d$ atom .....	30
V. Discussion .....	31
5.1. Problem of the excessive $\gamma$ quanta .....	31
5.2. Contribution of odd orbital angular momenta into annihilation in hydrogen and deuterium .....	32
VI. Conclusions. ....	34

## 1. Introduction

During the last years various experimental data were obtained (see reviews [1,2] ) showing the existence of nuclear-like bound and resonant states in nucleon-antinucleon system (so called quasinuclear mesons) predicted by Shapiro and co-workers (see reviews [3] ). One of the most impressive direct evidence for the existence of  $N\bar{N}$  mesons is the observation of the discrete spectrum of  $\gamma$  quanta in  $\bar{p}d$  annihilation [4] , though this result needs confirmation with better statistics. An important indirect evidence in favour of  $N\bar{N}$  states near threshold comes from a great contributions of nonzero orbital angular momenta into antiproton annihilation at rest [5,6,7] . Both these experimental facts need for their explanation the investigation of the process of  $\bar{p}$  capture in hydrogen and deuterium.

This paper is concerned with the analysis of stopping antiproton annihilation in liquid hydrogen and deuterium. After capturing into an atomic orbit the antiproton cascades down and finally annihilates from atomic or quasinuclear level. For  $\pi^-$  and  $K^-$  mesons the cascades have been investigated in detail by Leon and Bethe [8] , as to antiprotons, it has not been done for the lack of knowledge of  $N\bar{N}$  interaction necessary to determine the complex displacements of the atomic levels. According to the rough calculation done for  $\bar{p}p$  atom in the Ball-Chew model annihilation takes place from the states with zero orbital angular momenta [9] . The experimental data which are available now [4-7] and those which are expected in the nearest future [10-13] need the detailed

analysis of the cascade in  $\bar{p}$  atoms. The basic point of the present work is the relation between the atomic widths and the characteristic parameters of quasinuclear mesons such as their masses, widths and radii. The theoretical values of these parameters may vary in a rather wide range [1,14] and we pay great attention to that how these parameters affect the characteristic properties of the antiprotonic cascade, namely: the fractions of  $\bar{p}$  captured from the atomic orbits with different orbital angular momenta, the number of transitions from the atomic states into the quasinuclear ones, the intensity of the radiative transitions between the atomic levels. All the regularities and features of  $\bar{p}p$  and  $\bar{p}d$  atomic cascades are demonstrated by means of detailed calculations.

## II. De-excitation Processes

The formation and de-excitation of  $\bar{p}$  atoms in liquid hydrogen and deuterium are similar to  $N^-$  and  $K^-$  atoms [8,15]. The summary of the corresponding results valid for antiprotons is given below.

When the antiproton is slowed down to the velocity of about  $10^{-4}c$  it gets captured and as a result the  $\bar{p}p$  atom is formed with principal quantum number  $n \approx \sqrt{M} \approx 30$  ( $M$  is the reduced mass of  $\bar{p}p$  atom, atomic units are used throughout in all formulae  $\hbar = e = m_0 = 1$ ). At such high  $n$  stage the main de-excitation process is the chemical reaction  $\bar{p}p^{**} + H_2 \rightarrow \bar{p}p^* + H + H$ . The  $\bar{p}p$  atom loses  $\gg 4.5$  eV in this molecular dissociations and comes out with about one eV in kinetic energy, i.e. with the velocity of about  $10^6$  cm-sec $^{-1}$ . The cross section for this process drops off with  $n$  decreasing; it can be estimated by the formular [8]

$$\sigma^{chem} \approx \frac{1}{2} \pi a_n^2 \quad (1)$$

$a_n$  being the  $n$ -th Bohr radius of  $\bar{p}p$  atom.

At the  $n \leq 20$  stage the Auger ionization of the neighboring hydrogen atoms becomes the most important. The Auger de-excitation rate calculated in the Born approximation is [8]

$$\Gamma_{n'n}^{Auger} = N \frac{16\pi}{3M^2} R_{n'n}^2 (2\Delta E + 1.39)^{-\frac{1}{2}} \quad (2)$$

where  $N = 3.8 \cdot 10^{22} \text{ cm}^{-3}$  is the density of hydrogen atoms (for deuterium  $N = 4.2 \cdot 10^{22} \text{ cm}^{-3}$ ),  $R_{n'n}$  is the average (hydrogen) radial matrix element,  $\Delta E = E_n - E_{n'} - E_{ion}$  is the released energy ( $E_{ion} = 15.4 \text{ eV}$  is the molecular ionization energy). The resulting Auger rates for  $\bar{p}p$  and  $\bar{p}d$  atoms are presented in Table 1. Note, that the most intensive Auger transitions are with as little change in  $n$  as is consistent with supplying the  $H_2$  ionization energy.

The radiative de-excitation plays a role only at  $n \leq 4$  levels, the atomic radiation rates being equal to

$$\Gamma_{n'n}^{rad} = \frac{4}{3} \left( \frac{\Delta E_{n'n}}{c} \right)^3 \frac{R_{n'n}^2}{M^2} \quad (3)$$

### III. Widths of the atomic levels and annihilation rates

The annihilation rates of  $\bar{p}$  atom depend on the annihilation widths of the atomic levels and on the rates of their population due to the de-excitation processes and to the Day-Snow-Sucher mechanism [16]. The latter is the Stark

mixing of orbital angular momentum states which is induced when the  $\bar{p}$  atom passes through the electric field of neighboring hydrogen atoms. In this situation the annihilation rates are called the effective S-state annihilation rate or the effective P-state annihilation rate depending on what angular momentum state annihilation takes place from. It will be shown below that one may neglect annihilation from  $l > 1$  states.

### 3.1. Atomic widths

Apart from the Coulomb forces there is strong interaction in  $\bar{p}$  atom which can be considered as a perturbation because the range of nuclear interaction is much smaller than the atomic dimensions. By supposing the quantity  $\chi\sigma$  ( $\chi$  being the relative velocity,  $\sigma$  the annihilation cross section) to be represented as a sum of terms corresponding to quasinuclear states we can obtain the annihilation width

$\Gamma_{nl}^{ann}$  of the atomic  $nl$  level and estimate the value of its shift  $E_{nl}$  using the quasinuclear meson parameters [1].

The calculation of the graph for the mass operator presented in Fig. 1 gives

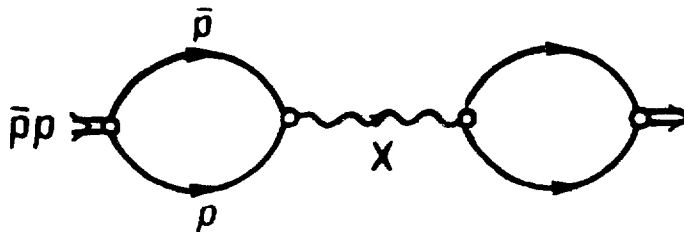


Fig. 1



$$E_{nl} - i \frac{\Gamma_{nl}}{2} = \frac{E^2}{E + i\Gamma/2} \left[ \int \Psi_{nl}(\vec{k}) \varphi_l(\vec{k}) d^3\vec{k} \right]^2 =$$

$$= \frac{E^2}{E^2 + \Gamma^2/4} (E - i\Gamma/2) g_{nl}^2 \quad (4)$$

where  $\Psi_{nl}(\vec{k})$  is the Coulomb wave function of the atom in the  $nl$  state and  $\varphi_l(\vec{k})$  is the wave function of the quasinuclear meson with the binding energy  $\Delta$ , the width  $\Gamma$ , and orbital angular momentum  $l$  ( $E \gg E_n$  - atomic binding energy). Let  $R_l$  be the  $\bar{N}\bar{N}$  meson linear dimension (usually  $R_l \approx 1$  fm) and  $a$  be the first Bohr radius of  $\bar{p}$  atom ( $a_{p\bar{p}} = 37.5$  fm,  $a_{p\bar{d}} = 40$  fm). Then the square of the overlapping integral  $g_{nl}^2$  is estimated by the formula [1]

$$g_{nl}^2 = \begin{cases} \frac{1}{n^3} \left( \frac{R_l}{a} \right)^3, & l=0 \\ \frac{n^2-1}{n^5} \frac{32}{3} \left( \frac{R_l}{2a} \right)^3, & l=1 \end{cases} \quad (5)$$

Our estimation of the atomic shifts is in agreement with the results of the exact numerical calculation [17] according to which the atomic levels are displaced up ( $E_{nl} > 0$ ) and the energy shifts are strongly spin-dependent.

The displacement of the  $\bar{p}d$  atomic level is determined by the graph presented in Fig. 2

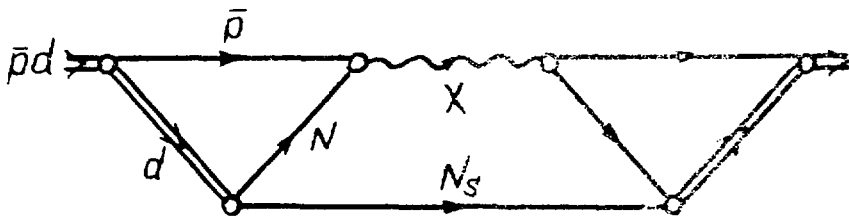


Fig. 2

Thus,

$$E_{nl} - i \frac{\Gamma_{nl}^{ann}}{2} = \int \frac{d^3 \vec{q}}{E - \frac{3q^2}{4m} + i \frac{\Gamma}{2}} \quad \times \quad (6)$$

$$\times \left[ \int d^3 \vec{k} \Psi_{nl}(\vec{k}) \Psi_d \left( \frac{\vec{k}}{2} + \vec{q} \right) \Psi_{l'} \left( \vec{k} + \frac{\vec{q}}{2} \right) \frac{\left( \frac{\vec{q}}{2} + \vec{k} \right)^2 + mE}{m} \right]^2$$

Setting  $l = l'$  and using the Hulthén deuteron wave function we get the estimation

$$\Gamma_{nl}^{ann} \approx -2 \gamma m E \frac{q_n^2}{g_{nl}^2} \int \frac{d^3 \vec{q} \Psi_d^2(\vec{q})}{E - \frac{3q^2}{4m} + i \Gamma/2} \approx \quad (7)$$

$$\approx g_{nl}^2 \left[ \frac{E^2}{\left( E - \frac{3q_n^2}{4m} \right)^2 + \Gamma^2/4} \Gamma + \frac{2\sqrt{3EE_d}}{\left( 1 + \frac{4}{3} \frac{mE}{\beta^2} \right)^2} \right]$$

Here  $\Psi_d(\vec{q})$  is the deuteron wave function,  $E_d = 2.22$  MeV being the deuteron binding energy,  $q_n$  is the effective momentum of the spectator nucleon  $N_s$  ( $q_n \approx 150$  MeV/c),  $\beta = 250$  MeV/c is the Hulthén parameter.

The graph in Fig. 2 contains two processes. One of them (the first term in square brackets in formula (7)) is the direct annihilation in the atomic orbits of  $\bar{p}N$  system with the effective mass  $M_{eff} = 2m - \frac{3q_n^2}{4m}$ . The other (the second term in square brackets in (7)) is the decay of the  $\bar{p}d$  atom into a nucleon and a quasinuclear meson. In this ca-

se both the nucleon  $N_S$  and the meson  $X$  are on the mass shell.

In fact there must be a sum over the quasinuclear mesons with different isospins in the right sides of formulae (4) and (6-7), for  $\bar{p}p$  atom each meson weighted with the factor of  $1/2$  (here the  $I = 0$  and  $I = 1$  states are equally probable) and for  $\bar{p}d$  atom the  $I = 0$  mesons weighted with the factor of  $1/2$  and the  $I = 1$  mesons with the factor of  $3/2$  (the  $\bar{p}n$  system has isospin  $I = 1$ ).

With orbital angular momentum  $l$  increasing the annihilation widths decrease rapidly according to the  $(R/a)^{5+2l}$  law (see (5)), therefore one may consider the annihilation from  $l = 0$  and  $l = 1$  states only.

The estimation given by the formula (7) takes into account the contributions from the quasinuclear states with the same value of orbital angular momentum as the atomic one. In case of  $\bar{p}d$  atom the antiproton-nucleon angular momentum can be different from the angular momentum of the antiproton with respect to the deuteron center of mass. Therefore there are the P-wave annihilation from S-orbitals and the S-wave annihilation from P-orbitals [7]. Let  $\Gamma_{nS(P)}^{ann}$  be the P-wave annihilation width from S-orbitals and similarly  $\Gamma_{nP(S)}^{ann}$  be the S-wave annihilation width from P-orbitals. As before this quantities are assumed to be determined correspondingly by P and S quasinuclear states. The following estimations are valid (with  $E \gg \Gamma$ ,  $E \gg q_n^2/m$ )

$$\Gamma_{nS(P)}^{ann} \approx \frac{\Gamma_P}{12} \left( \frac{R_P}{na} \right)^3 R_P^2 \langle q^2 \rangle_d \quad (8)$$

$$\Gamma_{nP(S)}^{ann} \approx \frac{\Gamma_S}{36} \left( \frac{R_S}{na} \right)^3 \frac{\langle z^2 \rangle_d}{a^2} \quad (9)$$

Here  $\langle q^2 \rangle_d \approx (110 \text{ MeV}/c)^2 \approx 0.3 \text{ fm}^{-2}$  and  $\langle r^2 \rangle_d \approx 4 \text{ fm}^2$  are the mean square relative momentum and radius of the deuteron. Now by comparison of (8) with (7) and (5) we can estimate the P/S ratio for annihilation from S-orbitals in  $\bar{p}d$  atom. By the order of magnitude this ratio is

$$\frac{\Gamma_{nS(P)}^{ann}}{\Gamma_{nS}^{ann}} \approx \frac{\Gamma_P}{12\Gamma_S} \left( \frac{R_P}{R_S} \right)^3 R_P^2 \langle q^2 \rangle_d \quad (10)$$

For the S/P ratio for P-orbitals we have the estimation

$$\frac{\Gamma_{nP(S)}^{ann}}{\Gamma_{nP}^{ann}} \approx \frac{\Gamma_S}{12\Gamma_P} \left( \frac{R_S}{R_P} \right)^3 \frac{\langle r^2 \rangle_d}{R_P^2} \quad (11)$$

From the above estimations one can see that if the radius of quasinuclear P-state is large ( $R_P \approx 3-4 \text{ fm}$ ) the P-wave annihilation from S-orbitals will compete with the S-wave one and be dominant for P-orbitals. The comparison of P-wave annihilation rates from S- and P-orbitals is not so straightforward because it requires the data on the relative population and depletion of S- and P-orbitals.

We are mainly interested in the dependence of the cascade processes on the quasinuclear mesons parameters and we do not pretend to the complete picture of the cascade. For this reason in performing the detailed calculations we shall ignore the P-wave annihilation from S-orbitals and S-wave annihilation from P-orbitals.

Besides annihilation there is another process which determines the atomic widths, namely the radiative transitions into quasinuclear states. The radiative width  $\Gamma_{nS}^\gamma$  of the atomic  $nS$  level due to radiative E1 transitions into quasinuclear P levels can be estimated as follows

$$\Gamma_{nS}^{\gamma} = \frac{\alpha}{4} \frac{1}{n^3} \left( \frac{\bar{R}_p}{a} \right)^3 \left( \frac{\omega \bar{R}_p}{c} \right)^2 \omega N_{\gamma} \quad (12)$$

Here  $\omega$  is the average  $\gamma$  energy ( $\omega \sim 100$  MeV),  $N_{\gamma}$  is the number of quasinuclear P-states ( $N = 8$  for the OREP version considered in [1,3]),  $\bar{R}_p$  is the average radius of quasinuclear P-states ( $\bar{R}_p \approx 1$  fm).

The exact value of the radiative width calculated with realistic wave functions may differ from the one given by (12). Then all the subsequent estimations based on the formula (12) have not to be considered too literally.

The ratio of  $\gamma$  transition probability  $P_{nS}^{\gamma}$  to the annihilation probability  $P_{nS}^{ann}$  is independent of  $n$ . With the values of all parameters being fixed after the equation (12) and  $R_S \approx \bar{R}_p \approx 1$  fm, the estimation for this ratio is given by

$$\frac{P_{nS}^{\gamma}}{P_{nS}^{ann}} = \frac{\Gamma_{nS}^{\gamma}}{\Gamma_{nS}^{ann}} \sim \frac{0.4 \text{ MeV}}{\Gamma_S} \quad (13)$$

$\Gamma_S$  being the quasinuclear S-state width.

The radiative width of nP level due to  $\gamma$  -transitions into quasinuclear S levels can be estimated by (supposing here again  $R_S \approx \bar{R}_p$ )

$$\Gamma_{nP}^{\gamma} \sim \left( \frac{R_S}{a} \right)^2 \Gamma_{nS}^{\gamma} \quad (14)$$

From (13), (14), and the equation for P-waves similar to (13) the ratio of  $\gamma$  transition probability from nP atomic level to the same quantity from nS level can be obtained

$$\frac{P_{nP}^{\gamma}}{P_{nS}^{\gamma}} = \frac{\Gamma_{nP}^{\gamma}}{\Gamma_{nP}^{ann}} \frac{\Gamma_{nS}^{ann}}{\Gamma_{nS}^{\gamma}} \frac{P_{nP}^{ann}}{P_{nS}^{ann}} = \left( \frac{R_S}{R_P} \right)^5 \frac{\Gamma_S}{\Gamma_P} \frac{P_{nP}^{ann}}{P_{nS}^{ann}} \quad (15)$$

Below we shall see that from the physical point of view the most interesting case is when  $P_P^{ann} \sim P_S^{ann}$ . This relation will be shown to hold under the condition  $\left( \frac{R_S}{R_P} \right)^5 \Gamma_S / \Gamma_P \ll 1$ , i.e. in this case the  $\gamma$ -transitions from P-levels can be ignored.

### 3.1. Stark mixing

An important role in the cascade process belongs to Stark mixing which was investigated in detail by Leon and Bethe for  $\text{Jl}^-$  and  $\text{K}^-$  atoms [8]. The similar treatment for  $\bar{p}p$  and  $\bar{p}d$  atoms is given below.

To calculate the Stark mixing rate  $\bar{p}$  atom is supposed to move with a constant velocity  $\vec{v}$  along an undeflected trajectory through the electric field of a fixed hydrogen atom. The transition probability between the states with orbital angular momenta  $l$  and  $l'$  as a function of impact parameter  $\rho$  is found by integrating the Schrödinger equation. At the beginning the states of given  $n$  are assumed to be degenerated, i.e. the energy displacement of the atomic levels due to the strong interaction is neglected.

The axis of quantization  $z$  is taken in the direction of the electric field  $\vec{E}$ , and  $y$  axis is orthogonal to the plane of vectors  $\vec{E}$  and  $\vec{v}$ . The wave function of  $\bar{p}$  atom is expanded into an orthonormal set of the Coulomb Hamiltonian eigenfunctions which are time dependent through the direction of the quantization axis  $z$  :

$$\Psi(t) = \sum_{l m} a_{l m}(t) \Psi_{n l m}$$

(the transitions between the states of different  $n$  being ignored here). Then from the Schrödinger equation one gets

$$i \dot{a}_{l m} + \dot{\theta} L_y a_{l m} = \sum_{l' m'} V_{l m l' m'} a_{l' m'} \quad (16)$$

where  $V_{l m l' m'} = \mathcal{E}(z) \langle l m | z | l' m' \rangle$ ,  $\mathcal{E}(z) = e^{-2z} \frac{2z^2 + 2z + 1}{z^2}$  is the strength of the electric field produced by a hydrogen atom at distance  $r$ ,  $\theta$  is the angle between  $\vec{\mathcal{E}}$  and  $\vec{z}$ . Dropping the  $\dot{\theta}$  term produces the "fixed field model" [8], then

$$i \dot{a}_{l m} = \sum_{l' m'} V_{l m l' m'} a_{l' m'} \quad (17)$$

This equation is separated in parabolic coordinates:

$$i \dot{a}_{n, m} = V_{n, m} a_{n, m} \quad (18)$$

Here  $V_{n, m} = \frac{3}{2} n(n_1 - n_2) \mathcal{E}(z) / M$ ,  $n_1$  and  $n_2$  are the parabolic quantum numbers ( $n_1 + n_2 + |m| + 1 = n$ ). Eq. (18) is easy to integrate

$$a_{n, m}(t) = a_{n, m}(-\infty) \exp \left\{ -i \int_{-\infty}^t V_{n, m}(\tau) d\tau \right\} \quad (19)$$

The transition probability  $P(l m, l' m', n, \rho)$  between the  $(l m)$  and  $(l' m')$  angular momentum states for a collision with

the impact parameter  $\rho$  is given by [8]

$$P(lm, l'm', n, \rho) = \delta_{mm'} \left| \sum_{j=-\frac{n-1}{2}}^{\frac{n-1}{2}} C_{\frac{n-1}{2} j \frac{n-1}{2} m-j}^{lm} C_{\frac{n-1}{2} j \frac{n-1}{2} m-j}^{l'm'} e^{i\varphi_{jn}} \right|^2 \quad (20)$$

$\varphi_{jn}(\rho)$  being the accumulated phase

$$\varphi_{jn}(\rho) = \frac{3n(2j-m)}{2M} \xi(\rho) \quad (21)$$

where

$$\xi(\rho) = \int_0^{\pi/2} d\theta e^{-2\rho \sec \theta} (1 + 2\rho \sec \theta + 2\rho^2 \sec^2 \theta) \quad (22)$$

Using Lie algebra methods approximate solutions for the Stark mixing were found allowing for turning of the  $z$  axis [18], in particular, one of them for  $P(00, 00, n, \rho)$  gives Eqs. (20)-(21) with  $\xi(\rho)$  defined as

$$\xi(\rho) = \int_0^{\pi/2} \cos \theta d\theta e^{-2\rho \sec \theta} (1 + 2\rho \sec \theta + 2\rho^2 \sec^2 \theta) \quad (23)$$

The functions  $P(00, 00, n, \rho)$  are presented for  $n = 5, 10, 20$  in Fig. 3. After the impact parameter  $\rho$  has reached the threshold value  $\rho_n$ , the probability  $P(00, 00, n, \rho)$  to stay in S-state increases rapidly approaching 1 that means the Stark mixing between the  $l = 0$  and  $l > 0$  states to be brought to stop.



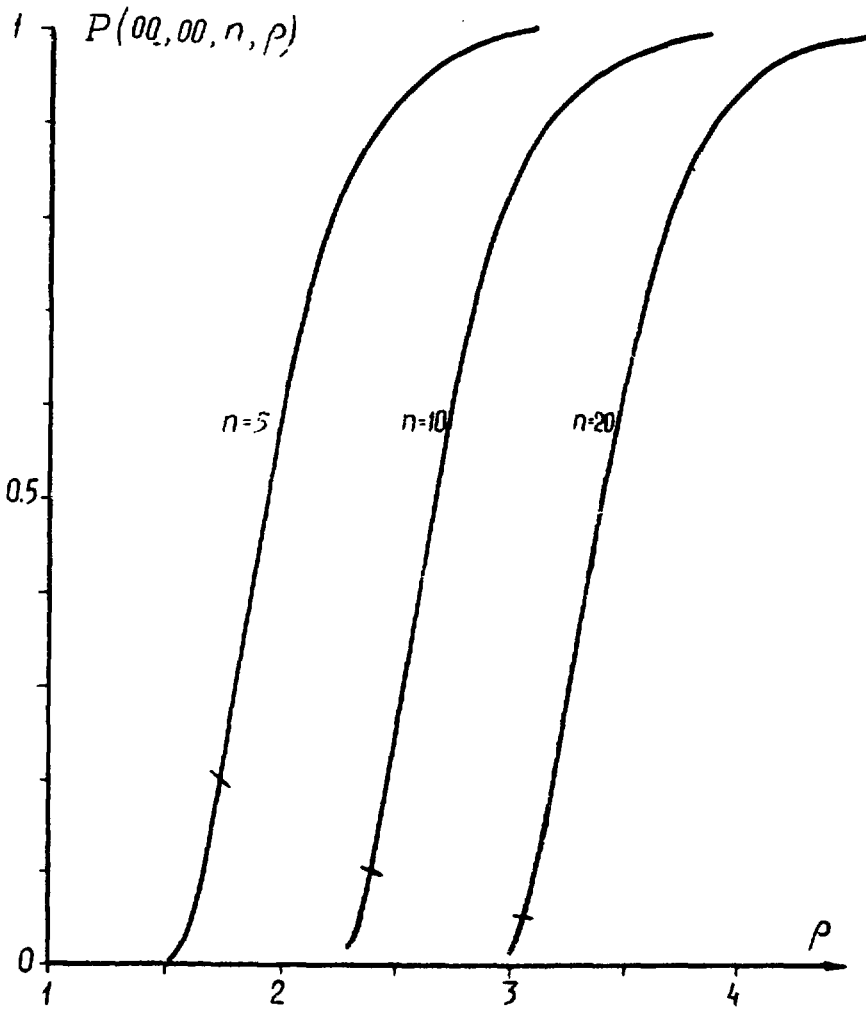


Fig. 3. Probability to stay in the  $nS$  state after the Stark collision v.s. impact parameter for  $\bar{p}p$  atom ( $v = 10^6 \text{ cm}\cdot\text{sec}^{-1}$ ).

Taking into account that in the fixed field model the S-state is mixed only with the  $m = 0$  states, the dimension of the region of the intense Stark mixing for the  $nS$  state,  $\rho_n$ , is defined as the root of the equation  $P(00, 00, \rho, n) = 1/n$ . The resulting  $\rho_n$  values are presented as a function of  $n$  in Fig. 4 for different atomic velocities.

By calculating the probabilities  $P(1m, \ell m', n, \rho)$  one gets then the dimension of the region of the Stark mixing for the  $nP$  state,  $\rho'_n$ . It appears that  $\rho'_n \approx \rho_n$ .

The realistic case differ from that considered above due to nuclear interaction. To take it into account one uses the fixed field model with S-state being shifted by  $E_{nS} - i\Gamma_{nS}/2$  due to strong interaction [8]. Then the Shrödinger equation yields

$$i\dot{a}_{n_1} = V_{n_1} a_{n_1} + \left( E_{nS} - i \frac{\Gamma_{nS}}{2} \right) \langle n_1 | \ell=0 \rangle \sum_{n'_1} \langle \ell=0 | n'_1 \rangle \quad (24)$$

Let  $\{a_{n_1}\}$  be an eigenvector with eigenvalue  $\lambda$ .

Then Eq. (24) gives

$$a_{n_1} = \frac{E_{nS} - i\Gamma_{nS}/2}{n(\lambda - V_{n_1})} \sum_{n'_1} a_{n'_1} \quad (25)$$

Summing over  $n_1$  and setting  $\gamma = \frac{2i(E_{nS} - i\Gamma_{nS}/2)M}{3En^2}$ ,  $\beta = \frac{\lambda M}{3En}$  one gets the eigenvalue equation for  $\beta$ :

$$\sum_{j=-\frac{n-1}{2}}^{\frac{n-1}{2}} \frac{1}{j-\beta} = \frac{2}{i\gamma} \quad (26)$$

When Stark splitting is much greater than the energy displacement ( $|\gamma| \ll 1$ ), the eigenvalues  $\lambda_k$  are

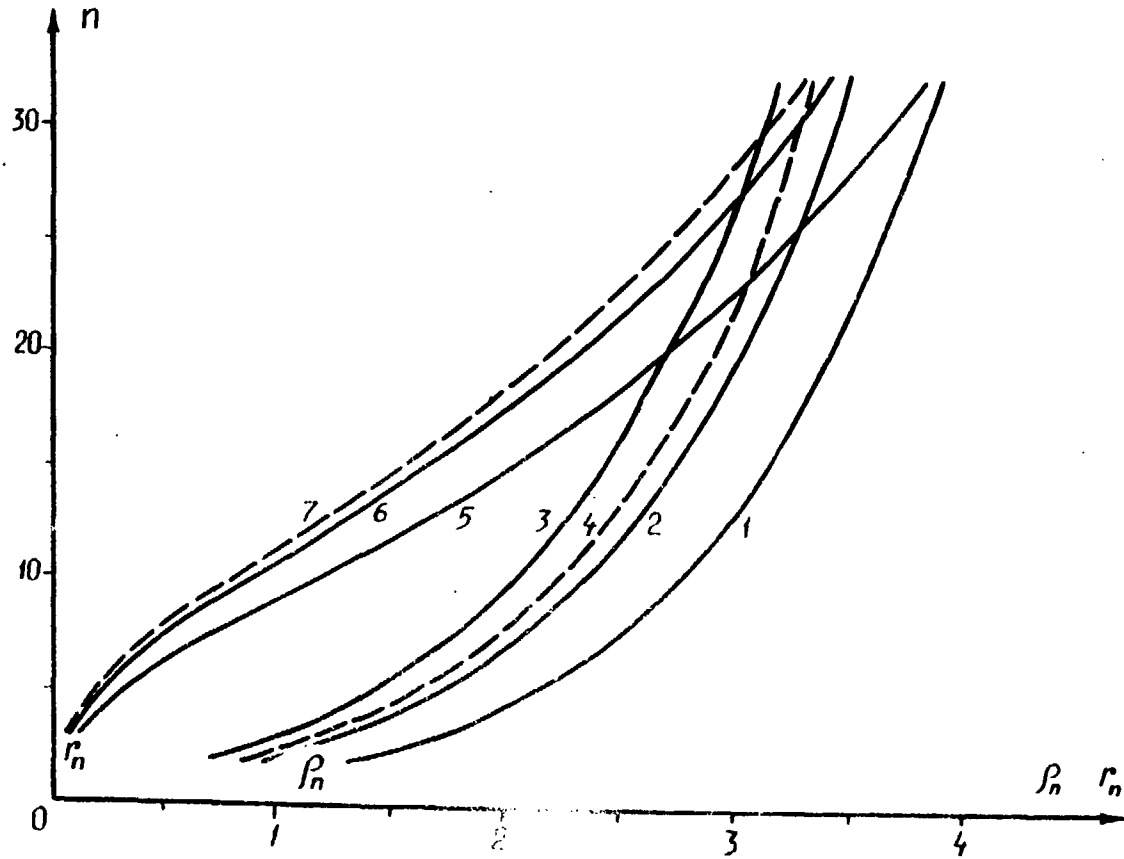


Fig.4. Effective impact parameter  $\rho_n$  for  $v=0.5 \cdot 10^6 \text{ cm} \cdot \text{sec}^{-1}$  (curve 1),  $10^6 \text{ cm} \cdot \text{sec}^{-1}$  (2,4),  $2 \cdot 10^6 \text{ cm} \cdot \text{sec}^{-1}$  (3) and effective radius  $r_n$  for the following parameters of quasinuclear mesons:  $\Gamma_q = 100 \text{ MeV}$ ,  $R_g = 1 \text{ fm}$  and atomic shifts  $E_{nS} = 2 \Gamma_{nS}$  (5,7),  $E_{nS} = 5 \Gamma_{nS}$  (6). Solid lines are for  $\bar{p}p$  atom, broken lines are for  $\bar{p}d$  atom.

$$\lambda_k = \frac{3\mathcal{E}n}{M} \left( \frac{n+1}{2} - k \right) + \frac{E_{nS} - i\Gamma_{nS}/2}{n}, \quad k=1, \dots, n \quad (27)$$

each eigenvector  $\{a_{n_i}^{(k)}\}$  containing the expected fraction  $1/n$  of the S-state. In this case the density matrix in the basis of the eigen vectors (the diagonal elements are kept only) has the form

$$\rho(t) = \frac{1}{n^2} \begin{pmatrix} \bar{I}_n e^{-\frac{\Gamma_{nS} t}{n}} & & \\ & & \\ & & \bar{I}_{n^2-n} \end{pmatrix}, \quad \text{Tr} \rho(0) = 1 \quad (28)$$

where  $\bar{I}_k$  is a unit matrix  $k \times k$ .

The annihilation probability during the time  $\tau$  is

$$A(\tau) = \bar{I}_2 \left( \rho(0) - \rho(\tau) \right) = \frac{1}{n} \left( 1 - e^{-\frac{\Gamma_{nS} \tau}{n}} \right) \quad (29)$$

The factor of  $1/n$  corresponds to the ignorance of Stark transitions between the states with different  $m$  in fixed field model. This model gives a lower limit for the effective annihilation rate.

At the other extreme of weak electric field ( $|\gamma| \gg 1$ ), one eigenstate is a slightly perturbed S-state. The other  $n - 1$  eigenstates contain a small admixture of the S-state; their average energy shift is

$$\bar{\lambda} \approx \frac{1}{3|\gamma|^2} \frac{E_{nS} - i\Gamma_{nS}/2}{n} \quad (30)$$

The density matrix in a corresponding basis has the form

$$\rho(t) = \frac{1}{n^2} \begin{pmatrix} I_1 e^{-\Gamma_{ns} t} & & \\ & I_{n-1} e^{-\frac{1}{3|\gamma|^2} \frac{\Gamma_{ns}}{n} t} & \\ & & I_{n^2-n} \end{pmatrix} \quad (31)$$

Then for the annihilation probability one gets

$$A(\tau) = \frac{1}{n^2} \left( 1 - e^{-\Gamma_{ns} \tau} \right) + \frac{n-1}{n^2} \left( 1 - e^{-\frac{1}{3|\gamma|^2} \frac{\Gamma_{ns}}{n} \tau} \right) \quad (32)$$

The first term in Eq. (32) is just the annihilation from S-state, and if there are no atoms in S-state, the second term should be kept only

$$A(\tau) \approx \frac{1}{n} \left( 1 - e^{-\frac{1}{3|\gamma|^2} \frac{\Gamma_{ns}}{n} \tau} \right) \quad (33)$$

An approximate formula for annihilation probability in arbitrary electric field was proposed in [8]:

$$A(\tau) = \frac{1}{n} \left( 1 - e^{-R \frac{\Gamma_{ns}}{n} \tau} \right) \quad (34)$$

where

$$R = \begin{cases} 1, & z \leq z_n \\ \frac{1}{3|\gamma|^2}, & z > z_n \end{cases} \quad (35)$$

Radius  $z_n$  is defined as a root of the equation  $3|\gamma(z_n)|^2 = 1$ . The resulting  $z_n$  values are presented as a function of  $n$  in Fig. 4 for various quasinuclear parameters.

In a wide range of  $n$ , from 1 to  $\sim 20$  the inequality

$\lambda_n < \rho_n$  holds true that means the dimension of the intense Stark mixing region is restricted by the strong field condition, i.e. by the distance at which the  $\bar{p}$  atom must come to the H atom for the Stark mixing to overcome the energy displacement of the S-state. Therefore, the effective S annihilation rate depends significantly on both the S level width of  $\bar{p}$  atom and its energy shift.

### 3.3. Effective annihilation rates

The effective P-state annihilation rate may be obtained as follows. Consider an  $\bar{p}$  atom moving along a straight line near the hydrogen atom. If  $\rho < \rho_n$ , the Stark collision involves the P-state in intensive mixing the time of which  $\tau_{St} \sim \rho_n / v$  is much smaller than the life-time of P-state ( $\Gamma_{nP}^{2M} \tau_{St} \ll 1$ ). Hence we may consider that P-state annihilation takes place between the Stark collisions. Then the effective P-state annihilation rate is given by the formula [19]

$$\Gamma_{nP}^{eff\ ann} = \frac{3}{n^2} \Gamma_{St} \left( 1 - e^{-\Gamma_{nP}^{2M} / \Gamma_{St}} \right) \quad (36)$$

here  $3/n^2$  is the statistical weight of nP state,  $\Gamma_{St}$  is the rate of Stark collisions:

$$\Gamma_{St} = \pi \rho_n^2 N v \quad (37)$$

In case of weak annihilation from P state ( $\Gamma_{nP}^{2M} \ll \Gamma_{St}$ ) we get

$$\Gamma_{nP}^{eff\ ann} = \frac{3}{n^2} \Gamma_{nP}^{ann}$$

The width of S level  $\Gamma_{nS} = \Gamma_{nS}^{ann} + \Gamma_{nS}^{\gamma}$  is so large that depletion is important during the collision. The fixed field model gives the lower limit for the effective S-state capture rate.

Before the collision the  $\bar{p}$  atom has  $m = 0$  with the probability  $1/n$ . The probability for this atom to pass through the region of intensive Stark mixing ( $\rho < \rho_n$ ) without being captured is  $\exp(-\int_{-\infty}^{+\infty} dx R(x) \frac{\Gamma_{nS}}{N\bar{z}})$  (integration is performed over the trajectory with the impact parameter  $\rho$ ,  $R(x)$  is defined by the formula (35)). After the collision the atom can be left in the S state (this probability being estimated by  $R(\rho)/n$ ) and then to be captured before the next collision with the probability  $(1 - \exp(-\frac{\Gamma_{nS}}{\tau_c}))$ ,  $\tau_c$  is the time elapsing between two collisions. As a result we receive for the effective S-state capture rate  $\Gamma_{nS}^{eff}$  the following formula (with  $\tau_c \gg 1/\Gamma_{nS}$ ) [8]:

$$\Gamma_{nS}^{eff} = \frac{N\bar{z}}{n} \int_0^{\rho_n} 2\pi \rho d\rho \left[ 1 - \left( 1 - \frac{R(\rho)}{n} \right) \times \right. \\ \left. \times \exp\left(-\int_{-\infty}^{+\infty} R(x) \frac{\Gamma_{nS}}{N\bar{z}} dx\right) \right] \quad (38)$$

The effective rates for annihilation and  $\gamma$ -transition from the S state are

$$\Gamma_{nS}^{eff\ ann} = \Gamma_{nS}^{eff} \frac{\Gamma_{nS}^{ann}}{\Gamma_{nS}} \quad (39)$$

$$\Gamma_{nS}^{\text{eff } \gamma} = \Gamma_{nS}^{\text{eff}} \frac{\Gamma_{nS}^{\gamma}}{\Gamma_{nS}} \quad (40)$$

#### IV. CASCADE CALCULATION

The detailed calculation has been made to search for the dependence of the capture schedule (fraction captured from S and P states, yields of  $\gamma$  accompanied annihilation) upon quasinuclear meson parameters. The capture schedule for  $\bar{p}p$  atom is given in Table 2 for the following set of parameters:  $\sqrt{S} = 100$  MeV,  $R_S = 1$  fm,  $E_{nS} = 2\sqrt{S}$ ,  $\sqrt{P} = 10$  MeV,  $R_P = 1$  fm. The Table contains the fraction  $P_n$  arriving in n state, the annihilation widths  $\Gamma_{nS}^{\text{ann}}$  and  $\Gamma_{nP}^{\text{ann}}$ , the effective rates  $\Gamma_{nS}^{\text{eff ann}}$  and  $\Gamma_{nP}^{\text{eff ann}}$ , the total rate  $\Gamma_n^{\text{eff}} = \Gamma_{nS}^{\text{eff ann}} + \Gamma_{nP}^{\text{eff ann}} + \Gamma_n^{\text{Auger}} + \Gamma_n^{\text{rad } nP} + \Gamma_n^{\text{chem}}$ , the fractions  $\rho_{nS}^{\text{ann}}$  and  $\rho_{nP}^{\text{ann}}$  annihilated in nS and nP states, the contribution  $\rho_{nS}^{\gamma}$  of radiative transitions between atomic nS levels and quasinuclear P states and the intensity of the atomic radiative transitions  $nP \rightarrow 1S$ . For  $\bar{p}d$  atom and the same values of quasinuclear parameters the corresponding rates are given in Table 3 ( $\rho_{nS}^d$  denotes the fraction captured in nS state due to  $\bar{p}d$  atom decay into a quasinuclear meson and a nucleon. The results of the cascade calculations for a wide range of the parameters  $E_S$ ,  $\sqrt{S}$ ,  $\sqrt{P}$ ,  $R_P$  are listed in Table 4. Below we discuss several regularities in S and P capture and  $\gamma$ -transitions.



#### 4.1. The S and P state capture sequence

There are two stages in the cascade process concerned; the first is the S capture stage, the other is the P capture one. The effective S state annihilation rate  $\Gamma_{nS}^{eff ann}$  has been shown to depend on the S level annihilation width growing with  $n$  decreasing and the Stark mixing rate which drops off when  $n$  becomes smaller. As a result, the rate  $\Gamma_{nS}^{eff ann}$  rises to a peak at  $n \sim 10$  for  $\bar{p}p$  atom and  $n \sim 14$  for  $\bar{p}d$  atom. In contrast to  $\Gamma_{nS}^{eff ann}$ , the effective P state annihilation rate is a monotonous function of level number. These two rates becomes equal at  $n \approx 3-8$  depending on quasinuclear parameters (Fig. 3).

The S annihilation stage includes the upper levels for which inequality  $\Gamma_{nS}^{eff ann} \gg \Gamma_{nP}^{eff ann}$  is valid. De-excitation via chemical processes and Auger effect for high  $n$  states goes on with a large change in  $n$ , so that after 4-5 transitions the atom starting from  $n = 50$  reaches  $n = 13-14$ . Later Auger transitions to the adjacent level predominates, their rate drops off much faster than does the S capture rate, so S absorption becomes more and more intensive. Later on S capture stage is replaced by the P capture one. This stage is defined by inequality  $\Gamma_{nP}^{eff ann} \geq \Gamma_{nS}^{eff ann}$ . The P capture fraction to a great degree depends on what extent S state absorption gives  $\bar{p}$  atom a chance to reach the P capture stage. If P capture stage sets in before the de-excitation rate decreases to the order of magnitude of  $\Gamma_{nS}^{eff ann}$ , then S state annihilation does not kill off most of the atoms and both S and P capture are significant. Otherwise as in the case of  $K^-$  and  $\pi^-$  mesoatoms S state annihilation

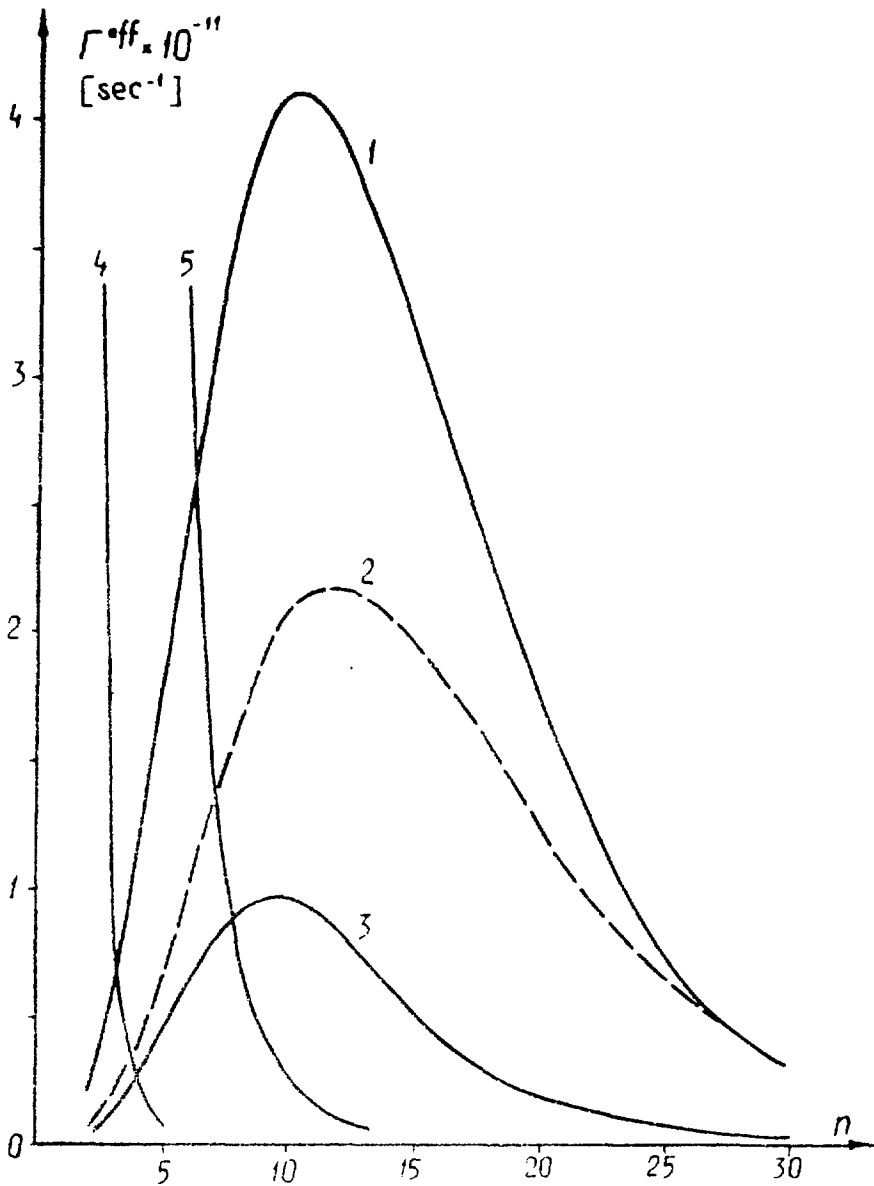


Fig. 5. Effective annihilation rate  $\Gamma_{nS}^{\text{eff ann}}$  for  $\bar{p}p$  atom for  $\sqrt{S} = 100$  MeV,  $R_S = 1$  fm,  $E_{nS} = 2\sqrt{nS}$  (curve 1),  $E_{nS} = \sqrt{nS}$  (2);  $\sqrt{S} = 10$  MeV,  $R_S = 1$  fm,  $E_{nS} = 20\sqrt{nS}$  (3) and  $\Gamma_{nP}^{\text{eff ann}}$  for  $\sqrt{p} = 10$  MeV,  $R_p = 1$  fm (4) and  $\sqrt{p} = 1$  MeV,  $R_p = 4$  fm (5) (everywhere  $v = 10^6$  cm·sec<sup>-1</sup>).

is dominant.

#### 4.2. The dependence on the widths of quasinuclear states

If the widths are large ( $\Gamma_S \sim 100$  MeV,  $\Gamma_P \sim 10$  MeV) and there is no P state with large radius located near threshold most of the atoms are captured during the S annihilation stage (see Table 4, NN 1, 10). The widths being smaller, the P capture stage is cut due to decreasing of effective rate of P annihilation but on the other hand the P stage is reached by larger amount of atoms because of previous S capture drop. For very small widths of quasinuclear states ( $\Gamma_S \sim 1$  MeV,  $\Gamma_P \sim 0.1$  MeV) the rates  $\Gamma_{nS}^{eff ann}$  and  $\Gamma_{nP}^{eff ann}$  are so small that P capture stage is absent, a substantial part of atoms ( $\sim 70\%$ ) arriving at  $n = 1$ . In this case radiation is of great importance, and the intensive radiative transitions can be observed between the lower atomic levels and from the atomic states into quasinuclear ones.

The average number of the excessive  $\gamma$  quanta per  $\bar{p}d$  annihilation act at rest equals to  $0.73 \pm 0.08$  [4]. If most of them is due to transitions between atomic  $nS$  levels and quasinuclear P levels, then according to formula (13) quasinuclear S states must be narrow [1]:

$$\Gamma_S \leq 0.4 \text{ MeV}$$

The other necessary condition for the excess of  $\gamma$  to be explained by this mechanism is that binding energies of S states should be of several hundreds MeV (more than one hundred), otherwise  $\gamma$  transitions will be suppressed by radiationless S capture process  $\bar{p}d \rightarrow X + N_S$ .

If the excess of  $\gamma$  corresponds to radiative transitions between quasinuclear levels, then the S states should also be narrow, but their binding energies should be smaller ( $E_S \lesssim 100$  MeV). In this case, the nuclear  $\gamma$ -radiation follows radiationless transitions from the  $\bar{p}d$  atomic level up to quasinuclear  $\overline{NN}$  level with nucleon-spectator emission, the radiative widths of quasinuclear states being comparable to annihilation ones.

#### 4.3. The dependence on the radius of quasinuclear P-state

If there is a bound  $\overline{NN}$  P state near threshold ( $E_P \sim 1-2$  MeV) with a large radius  $R_P \approx 3-4$  fm, the effective P state annihilation rate grows up significantly (see formula (5)). As a result, the P capture stage begins at relatively high levels (see Fig. 5), which are reached by large enough fraction of atoms, and P state capture is comparable with the S state one (compare N. 1 and N.4 in Table 4).

#### 4.4. The dependence on the energy displacement of the atomic S level

It follows from the given above Stark mixing process analysis that the greater is the energy displacement of the atomic S level, the smaller is the effective S state annihilation rate (see Fig. 5), and hence the greater is the fraction of P state annihilation (compare N.1 and N.7 in Table 4).

#### 4.5. The role of the velocity of $\bar{p}$ atom

The effective S state annihilation rate depends significantly on the Stark collisions frequency which is proportional to the velocity. Therefore, the less the velocity is, the larger is the fraction arriving at P capture stage, i.e. the greater is the P state contribution to annihilation (compare NN. 1,8, 9 in Table 4).

#### 4.6. The dependence on the reduced mass of $\bar{p}$ atom

Since the radii of the Bohr orbits in  $\bar{p}d$  atom are  $4/3$  times smaller than in  $\bar{p}p$  atom, the shifts and widths of its levels are greater according to formula (5). The S level displacement rising and  $\bar{p}d$  atom dimension decreasing result in a drop of the Stark mixing rate (see Fig. 4). Hence the ratio  $\frac{\Gamma_{nP}^{off\ am}}{\Gamma_{nS}^{off\ am}}$  for  $\bar{p}d$  atom is several times as large as that for  $\bar{p}p$  atom. Therefore the P capture stage spreads to higher n levels and P state annihilation increases in comparison with  $\bar{p}p$  atom (see Table 4).

#### 4.7. I-spin analysis

The complex energy displacement of  $\bar{p}p$  and  $\bar{p}d$  atomic levels depends on I-spin structure of these systems. As was discussed in 3.1. the contributions of isoscalar and isovector quasinuclear states in  $\bar{p}p$  atom are equal while in  $\bar{p}d$  atom the contribution of isovector mesons is three times greater than that of isoscalar ones. So the more important is the role of isovector quasinuclear P states, the more significant is the increase of the ratio  $\frac{\Gamma_{nP}^{off\ am}}{\Gamma_{nS}^{off\ am}}$  in  $\bar{p}d$  in comparison with  $\bar{p}p$  (see Table 5).

#### 4.8 Spin analysis

Spin is a "good" quantum number in the atomic processes concerned. The probability for  $\bar{p}p$  atom to be formed with  $S_a = 0$  is  $1/4$  and with  $S_a = 1$  is  $3/4$  and there are two independent cascades each being determined by singlet ( $S_N=0$ ) or triplet ( $S_N = 1$ ) quasinuclear mesons.

The  $\bar{p}d$  atom is formed with  $S_a = 1/2$  with probability equal to  $1/3$  and with  $S_a = 3/2$  with probability equal to  $2/3$ . The widths of  $S_a = 3/2$  atomic states are determined by triplet quasinuclear mesons only, whereas there are contributions from both triplet mesons weighted with the factor of  $1/4$  and from singlet mesons weighted with the factor of  $3/4$  to the  $S_a = 1/2$  atomic states widths. There is strong spin dependence of  $N\bar{N}$  interaction [3] and so the cascades for two different spin states will differ from each other.

#### 4.9. P capture from S orbitals in $\bar{p}d$ atom

Finally we would remind of P capture from S orbitals in  $\bar{p}d$  atom discussed above (see 3.1). This mechanism also increases the contribution of P state annihilation in  $\bar{p}d$  atom. It is very important in case there exists the P state with large radius ( $R_p \approx 3-4$  fm) near threshold. Then annihilation from S orbitals gives the main contribution to P state annihilation.

## V. DISCUSSION

### 5.1. Problem of the excessive $\gamma$ quanta

In the experiment of T.E.Kalogeropoulos and co-workers [4] it was shown that average energy taken away by charged pions produced in  $\bar{p}d$  annihilation is less than it is required by isotopical invariance. The excess of neutral energy is carried away by intensive hard gamma radiation which probably was proved to have discrete spectrum. It was found that 7% of  $\bar{p}d$  annihilations are accompanied by excessive  $\gamma$  quanta.

A possible explanation is that annihilation follows the radiative transitions from the atomic orbits into the quasinuclear states. In this case the upper limit to the excess of  $\gamma$  can be easily obtained. The necessary condition of intensive  $\gamma$  radiation has been shown to be the small enough annihilation widths of the quasinuclear S states. All the S states cannot be narrow, there must be a broad state which is responsible for the S wave annihilation amplitude. If the triplet ( $S = 1$ )  $I = 0$  states had been broad,  $\gamma$  radiation would have been suppressed by annihilation for any value of the  $\bar{p}d$  atom spin. But if the triplet S states are narrow, then the  $\gamma$  transitions from the atomic into quasinuclear levels will be the main process terminating the cascade in  $\bar{p}d$  atom with  $3/2$  spin. The statistical weight of the  $S = 3/2$  states is equal to  $2/3$ , i.e. the upper limit to the number of excessive  $\gamma$  accompanied  $\bar{p}d$  annihilation act is  $2/3$ . For  $\bar{p}p$  atom the similar value equals

to the statistical weight of the  $S = 1$  states, i.e.  $3/4$  <sup>1)</sup>.

The radiative transitions between quasinuclear states is another possible source of excessive  $\gamma$  radiation. Cascading between  $\overline{NN}$  quasinuclear levels occurs after the decay of  $\overline{pd}$  atom into nucleon and quasinuclear meson. Therefore if cascading between quasinuclear states is the main source of  $\gamma$  radiation then the yield of  $\gamma$  in  $\overline{pp}$  atom should be considerably smaller in comparison with  $\overline{pd}$  atom.

### 5.2. Contribution of odd orbital angular momenta into annihilation in hydrogen and deuterium

It follows from angular momentum and parity conservation that annihilation into two spinless bosons ( $2\pi$ ,  $2K$ ) is possible from triplet states of  $\overline{NN}$  system only. Besides that if bosons are identical (annihilation into  $2\pi^0$ ,  $2K_S$ ), the reaction results from  $\overline{NN}$  states with odd orbital angular momenta (P, F, etc.). So, the relative contributions of S and P waves into annihilation can be estimated by the ratio of annihilation cross sections  $\overline{NN} \rightarrow 2\pi^0$  to  $\overline{NN} \rightarrow \pi^+\pi^-$  or  $\overline{NN} \rightarrow 2K_S$  to  $\overline{NN} \rightarrow K_L K_S$ . The ratio of  $\overline{pp}$  two body pionic annihilation in hydrogen from the states with odd orbital angular momenta to the total two-body pionic annihilation cross section is [5]:

$$R_H(\pi) = \frac{\overline{pp} \Big|_{L=odd} \rightarrow 2\pi}{\overline{pp} \Big|_{L=all} \rightarrow 2\pi} = 0.39 \pm 0.08 \quad (41)$$

<sup>1)</sup> For  $\overline{pp}$  annihilation there is no general relation between numbers of charged and neutral pions



For deuterium the same ratio is equal to [6] :

$$R_D(\pi) = \frac{\bar{p}p)_{\ell=\text{odd}}^D \rightarrow 2\pi}{\bar{p}p)_{\ell=\text{all}}^D \rightarrow 2\pi} = 0.75 \pm 0.08 \quad (42)$$

Similar ratios for  $K^0\bar{K}^0$  channel are [7]

$$R_H(K) = \frac{\bar{p}p)_{\ell=\text{odd}}^H \rightarrow 2K}{\bar{p}p)_{\ell=\text{all}}^H \rightarrow 2K} = 0.015 \pm \begin{matrix} 0.012 \\ 0.005 \end{matrix} \quad (43)$$

$$R_D(K) = \frac{\bar{p}p)_{\ell=\text{odd}}^D \rightarrow 2K}{\bar{p}p)_{\ell=\text{all}}^D \rightarrow 2K} = 0.09 \pm 0.03 \quad (44)$$

Because additional hard  $\gamma$  quanta seem to have not been observed here, quantities (43)(44) relate to the processes going without preliminary electromagnetic transitions into quasinuclear P states.

If we assume the excessive  $\gamma$  quanta to be a result of radiative transitions between the atomic and quasinuclear levels then, as we have already shown, annihilation widths of triplet S states ( $l = 0, S = 1$ ) should be smaller than radiative ones. In this case annihilation probabilities from S and P states can be comparable. Such a picture is consistent with the experimental ratios  $R_H(\pi)$  and  $R_D(\pi)$  which are expected to reflect the contribution of S and P waves into total annihilation correctly, though they relate to the specific channel  $2\pi$ . Necessary to emphasize again that S and P waves contributions under discussion relate only to direct annihilation from atomic levels, but there is also P wave annihilation following  $\gamma$  transitions from atomic into quasinuclear levels. The relative magnitude of these two different P wave contributions is the other essential number necessary to take into account. Narrow  $\bar{3}S_1$  state can

ensure the excess of  $\gamma$  and the comparable probabilities of S and P state annihilation from atomic levels. But to obtain large absolute value of P state annihilation from atomic levels (i.e. comparable to P state annihilation following  $\gamma$  transitions) necessary to assume the existence of P state with large radius near threshold. Large radius is natural for a loosely bound state. Such radius would ensure high annihilation probability from atomic P states ( $\int_{r_0}^{\infty} |\psi|^2 r^2 dr \sim R_p^5$ , see formula (5)), but would not influence the probability of  $\gamma$  transitions from atomic into quasinuclear levels because of small transition energies. This conclusion on the role of P state with large radius is approved by detailed calculations (see Tables 4.5).

The ratio  $R_D(\pi)/R_H(\pi) \approx 2$  is in agreement with the increase of the P state annihilation fraction in  $\bar{p}d$  atom in comparison with  $\bar{p}p$  one that comes from smaller radius of  $\bar{p}d$  atom and from additional  $\bar{p}d$  interaction (see Secs. 4.7, 4.9). The similar ratio  $R_D(\kappa)/R_H(\kappa) \approx 6$  can be not equal to  $R_D(\pi)/R_H(\pi)$  because of possible interference effect in reaction  $\bar{p}p \rightarrow 2K_S$  (interference is between  $\bar{1}^6 = 0^+$  and  $1^-$  states) while in reaction  $\bar{p}p \rightarrow 2\pi^0$  this interference is absent (for details see [1, 20]).

## VI. CONCLUSIONS

We have shown by our investigation that the essential features of experimental data on the annihilation of antiprotons stopping in liquid hydrogen and deuterium can be explained by the existence of bound states in nucleon-antinucleon system. However additional experiments are needed to confirm the proposed physical picture and to clarify some am-

biguities. Besides the confirmation of the excess of  $\gamma$  with discrete spectrum accompanied  $\bar{p}d$  annihilation the following experiments are among the most important:

1) Investigation of  $\gamma$  spectrum accompanied  $\bar{p}p$  annihilation. The existence of the discrete  $\gamma$  spectrum accompanied  $\bar{p}p$  annihilation would mean that  $\gamma$  radiation in  $\bar{p}d$  annihilation is due to  $\gamma$  transitions between atomic and quasinuclear states <sup>1)</sup>. The absence of discrete lines in  $\bar{p}p$  annihilation and their presence at the same in  $\bar{p}d$  annihilation would mean that there are radiative transitions between quasinuclear levels; this transitions follows the decay  $\bar{p}d \rightarrow \chi + N$ . The other possibility is that  $\gamma$  with discrete spectrum in  $\bar{p}d$  annihilation is due to radiative transitions into three-body quasinuclear bound state  $\bar{p}n\bar{n}$  (for calculation of the spectrum of such states see references in [1]).

2) The investigation of spin dependence of energy shifts and widths of atomic levels. Such dependence can be studied by observation the splitting of the lines  $\bar{p}p \rightarrow \gamma$ . According to calculations [17] this splitting should be of the order of several hundreds eV. By measuring the widths of the lines it is possible to deduce whether the widths of quasinuclear states are really spin dependent. From the narrowness of  ${}^3S_1$  states hypothesis it follows that one of the lines (triplet) should be much more narrow than the other (singlet). The triplet line can be distinguished from the singlet one by observation of the products of annihilation.

Annihilation into two spinless bosons ( $2J\pi$ ,  $\pi\pi$ , etc.) can

<sup>1)</sup> In this case the lines in  $\bar{p}d$  atom would be broader in comparison with  $\bar{p}p$  atom due to emission of recoiling nucleon.

result only from triplet states.

3) If hard  $\gamma$  quanta with discrete spectrum in  $\bar{p}p$  annihilation will be observed, necessary to compare the probabilities of the processes  $\bar{p}p \rightarrow 2\pi^0$  and  $\bar{p}p \rightarrow 2\pi^0\gamma$  (with  $\gamma$  energy of the order of 100 MeV). By such a comparison it is possible to obtain the relation between probabilities of annihilation from atomic and quasinuclear P states and also to check the hypothesis of the existence of P states with large radius near threshold. Dominance of the process with additional  $\gamma$  emission would mean that the bulk of P state annihilation takes place after radiative transition from atomic into quasinuclear states; this would be the evidence in favour of the narrowness of  ${}^3S_1$  states. If the probabilities of both processes would be comparable, it would be the evidence in favour of the existence of P state with large radius near threshold.

Further investigations of  $\bar{p}p$  and  $\bar{p}d$  atoms are very important for the determination of the spectrum and quantum numbers of quasinuclear mesons and also for understanding of  $N\bar{N}$  interaction at small distances.

We wish to thank Professor I.S.Shapiro for many helpful discussions and comments on this work. We also take pleasure in acknowledging Dr. N.Ya.Smorodinskaya for her help in preparing this preprint.

## T A B L E S

- Tables 1A,B. Auger Rates for  $\bar{p}p$  atom (1A) and for  $\bar{p}d$  atom (1B) (in units of  $10^{10} \text{sec}^{-1}$ );  $n_i$  is the initial level,  $n_f$  is the final level,  $k$  is the least possible change in principal quantum number.
- Table 2. Cascade schedule for  $\bar{p}p$  atom ( $E_s = 200 \text{ MeV}$ ,  $\Gamma_s = 100 \text{ MeV}$ ,  $R_s = 1 \text{ fm}$ ,  $E_{nS} = 2 \sqrt{\Gamma_{nS}}$ ,  $\Gamma_p = 10 \text{ MeV}$ ,  $R_p = 1 \text{ fm}$ ,  $\omega = 100 \text{ MeV}$ ,  $N_\gamma = 8$ ,  $\beta = 10^6 \text{ cm} \cdot \text{sec}^{-1}$ ). Rates are in units of  $10^{10} \text{sec}^{-1}$ . Both spin and isospin dependence of the parameters of quasinuclear mesons is neglected.
- Table 3. Cascade schedule for  $\bar{p}d$  atom ( $E_s = 200 \text{ MeV}$ ,  $\Gamma_s = 100 \text{ MeV}$ ,  $R_s = 1 \text{ fm}$ ,  $E_{nS} = 2 \sqrt{\Gamma_{nS}}$ ,  $\Gamma_p = 10 \text{ MeV}$ ,  $R_p = 1 \text{ fm}$ ,  $\omega = 100 \text{ MeV}$ ,  $N_\gamma = 8$ ,  $\beta = 10^6 \text{ cm} \cdot \text{sec}^{-1}$ ). Rates are in units of  $10^{10} \text{sec}^{-1}$ . Both spin and isospin dependence of the parameters of quasinuclear mesons is neglected.
- Table 4. The dependence of the  $\bar{p}$  cascade (both for  $\bar{p}p$  and  $\bar{p}d$  atoms) on the parameters of quasinuclear mesons. Everywhere  $\Gamma_p = 0.1 \Gamma_s$ ,  $R_s = 1 \text{ fm}$ . The contribution of quasinuclear mesons into atomic widths are taken with unit weight both in  $\bar{p}p$  and  $\bar{p}d$ ,  $E_s / \Gamma_s = E_{nS} / \Gamma_{nS}$ .
- Table 5. Isospin dependence of  $\bar{p}$  cascade.

Table 1A

$n_i$	$n_i$		$n_i - k$	$n_i - k - 1$	$n_i - k - 2$
	$k$				
2	I		0.0072	-	-
3	I		0.249	0.0005	-
4	I		1.96	0.0166	0.00009
5	I		3.85	0.129	0.00336
6	I		16.6	0.555	0.026
7	I		73.4	1.73	0.112
8	I		164.	4.39	0.344
9	I		380.	9.69	0.864
10	I		608.	19.2	1.89
11	I		1047	35.3	3.72
12	I		1707	60.6	6.76
13	2		98.6	11.6	2.12
14	2		154	18.8	3.61
15	2		231	29.1	5.83
16	3		43.7	9.04	2.37
17	3		63.4	13.5	3.67
18	3		89.6	19.6	5.48
19	4		27.7	7.93	2.63
20	4		38.2	11.2	3.30
21	5		15.4	5.36	2.05
22	5		20.8	7.37	2.88
23	6		9.95	3.97	1.69
24	6		13.2	5.35	2.32
25	7		7.03	3.13	1.45

Table 1B

$n_i$	$n_i$		$n_i - k$	$n_i - k - 1$	$n_i - k - 2$
	$n_i$	$k$			
2	I	I	0.0039	-	-
3	I	I	0.188	0.0003	0.0005
4	I	I	1.07	0.0089	0.0018
5	I	I	4.74	0.069	0.014
6	I	I	15.2	0.297	0.066
7	I	I	39.4	0.926	0.184
8	I	I	88.5	2.34	0.465
9	I	I	178.	5.21	1.01
10	I	I	350	10.6	2.00
11	I	I	571	19.0	3.54
12	I	I	985	32.3	5.28
13	I	I	1461	50.1	7.94
14	I	I	2267	75.6	11.15
15	I	I	3426	105.9	15.89
16	I	I	5184	141.6	22.38
17	I	I	7661	190.7	30.97
18	I	I	11149	251.9	42.30
19	I	I	16392	320.9	57.09
20	I	I	24000	400.	76.09
21	I	I	34830	490.	99.16
22	I	I	49680	580.	128.16
23	I	I	69450	670.	164.91
24	I	I	95160	760.	211.70
25	I	I	128800	850.	274.70

Table 2

$n$	$P_n$	$\Gamma_n^{\text{eff}}$	$\Gamma_{nS}^{\text{ann}}$	$\Gamma_{nS}^{\text{eff ann}}$	$\Gamma_{nP}^{\text{ann}}$	$\Gamma_{nP}^{\text{eff ann}}$	$P_{nS}^{\text{ann}}$	$P_{nP}^{\text{ann}}$	$P_{nS}^{\text{eff}}$	$P_{nP \rightarrow nS}^{\text{eff}}$
30	1.0	169	2800	3.02	0.03	$9.7 \cdot 10^{-3}$	.019	$5.7 \cdot 10^{-7}$	$7.2 \cdot 10^{-5}$	
26	.951	112	4200	6.03			.051			
23	.770	81.5	6100	10.3			.098			
21	.524	75.5	8100	14.4			.049		$4 \cdot 10^{-4}$	
20	.017	102	9600	16.5			.003			
19	.354	83.5	1.1	19.4			.042			
18	.045	158	1.3	26.2			.016			
17	.226	122	1.5	25.1			.046			
16	.181	96.1	1.3	17.5	0.19	0.003	.053		$6.1 \cdot 10^{-4}$	
15	.472	307	1.2	36.9			.001			
14	.176	111	2.7	33.6			.001			
13	.116	175	3.4	36.5			.001			
12	.172	133	9.3	38.5			.001			
11	.332	125	5.6	40.6	0.6		.011		$5.5 \cdot 10^{-5}$	
10	.886	922	7.3	41.2			.001			
9	.307	332	1.6	46.2			.033			
8	.390	267	1.5	47.6			.059			
7	.274	101	1.2	37.2			.001			
6	.195	55.4	3.5	25.6			.001		$2.5 \cdot 10^{-4}$	
5	.106	29.0	9.0	1.3	0.1		.047			$2.3 \cdot 10^{-3}$
4	.086	10.5	1.2	11.3	11.6		.022			$1.5 \cdot 10^{-3}$
3	.0071	23.4	2.8	1.7	56		.001			$1.6 \cdot 10^{-3}$
2	.0036	10.3	9.3	3.0	75		.001			
1	.0053	7.5	107				.0056			
						<i>total</i>	0.943	1.010	0.604	



Table 3

A	$P_n$	$\Gamma_n^{off}$	$\Gamma_{NS}^{ann}$	$\Gamma_{NS}^{off ann}$	$\Gamma_{nP}^{ann}$	$\Gamma_{nP}^{off ann}$	$P_{NS}^{ann}$	$P_{nP}^{ann}$	$P_{NS}^{off}$	$P_{nP}^{off}$	$P_{NS}^d$	$P_{nP}^d$
80	1.0	128	1.3	13.4	0.25	$8.5 \cdot 10^{-4}$	0.108	$7 \cdot 10^{-6}$	$2.2 \cdot 10^{-4}$	0.0038		
26	.802	93.4	2.0	17.8	0.74	$5.0 \cdot 10^{-8}$	0.152	$1.8 \cdot 10^{-5}$	$1 \cdot 10^{-4}$	0.0019		
28	.478	79.4	3.0	21.8								
22	.491	106.0	3.4	23.4								
21	.280	89.0	3.9	24.9								
20	.180	166	4.5	26.0								
19	.105	132	5.2	28.0								
18	.156	103	2.2	29.4								
17	.202	245	7.8	30.6								
16	.113	253	8.8	31.4								
15	.258	184	1.06	31.9								0.043
14	.150	133	1.31	31.8			0.031					
13	.197	1556	1.64	31.0			0.0039					
12	.291	1004	2.08	29.5			0.0085					
11	.292	622	2.70	27.2	5.12	0.13	0.013	$6 \cdot 10^{-5}$	$2.5 \cdot 10^{-5}$	0.0004		
10	.281	368	3.60	24.3			0.019					
9	.268	206	4.98	20.8			0.026					
8	.287	110	7.02	17.0			0.037					
7	.200	55.6	1.05	13.2			0.047					
6	.149	23.8	1.66	9.49	50.2	2.14	0.050	0.013	$1 \cdot 10^{-4}$	0.0015		
5	.085	18.4	2.87	8.22	58.7	6.14	0.029	0.028				
4	.026	25.7	5.61	3.57	101	17.4	0.0036	0.018				
3	.0048	70.0	1.38	1.66	226	57.8	0.0001	0.0036				
2	.0028	169	4.49	0.42	644	151	0.0024	0.0024				
1	.0021		35.9				0.0021					
							0.899	0.072	0.002	0.027		
					<i>total</i>							

Table 4

$N^{\beta}$	$\Gamma_S$	MeV	$E_{n\beta}/\Gamma_{n\beta}$	$R_p$ fm	$\delta$ cm sec <sup>-1</sup>	$P_{n\beta}^{dini}$	$P_{n\beta}^{dini}$	$P_{n\beta}^{dini}$	$P_{n\beta}^{dini}$	$P_{n\beta}^{dini}$
$\bar{p}p$ atom										
I		100	2	I	10 <sup>6</sup>	0.968	0.013	0.004	-	-
2		10	20	I	10 <sup>6</sup>	0.929	0.036	0.035	-	-
3		I	200	I	10 <sup>6</sup>	0.718	0.012	0.270	-	-
4		100	2	4	10 <sup>6</sup>	0.724	0.273	0.003	-	-
5		10	20	4	10 <sup>6</sup>	0.343	0.644	0.013	-	-
6		10	5	4	10 <sup>6</sup>	0.577	0.401	0.022	-	-
7		100	5	I	10 <sup>6</sup>	0.920	0.076	0.004	-	-
8		100	2	I	5·10 <sup>6</sup>	0.969	0.027	0.004	-	-
9		100	2	I	2·10 <sup>6</sup>	0.989	0.007	0.004	-	-
$\bar{p}d$ atom										
10		100	2	I	10 <sup>6</sup>	0.927	0.041	0.004	0.028	0.028
11		10	20	I	10 <sup>6</sup>	0.663	0.122	0.024	0.191	0.191
12		10	20	4	10 <sup>6</sup>	0.251	0.669	0.009	0.071	0.071
13		10	5	4	10 <sup>6</sup>	0.359	0.304	0.014	0.323	0.323
14		100	5	I	10 <sup>6</sup>	0.807	0.183	0.003	0.007	0.007

Table 5.

MESON PARAMETERS	ISOSPINS OF MESONS	$\rho_{pp}$ ns	$\rho_{pn}$ np	$P_Y$ ns	$P_d$ ns	INTENSITIES OF ATOMIC TRANSITIONS
$E_s = 200 \text{ MeV}$ $r_s = 100 \text{ MeV}$ $R_B = 1 \text{ fm}$ $r_p = 10 \text{ MeV}$ $R_p = 1 \text{ fm}$ $E_{ns} = 2 \text{ MeV}$ $\omega = 100 \text{ MeV}$ $N_Y = 8$ $\beta = 10^6 \text{ cm}\cdot\text{sec}^{-1}$	I = 1	.987	.005	.008	-	$4P \rightarrow 1S \quad 1.4 \cdot 10^{-3}$ $3P \rightarrow 1S \quad 1.1 \cdot 10^{-3}$
		I = 1 and I = 0	.909	.060	.003	.028
	I = 1 and I = 0		.983	.013	.004	-
		I = 1 and I = 0	.899	.072	.002	.027
	I = 1		.417	.551	.032	-
		I = 1 and I = 0	.318	.586	.008	.088
	I = 1 and I = 0		.343	.644	.013	-
		I = 1 and I = 0	.234	.696	.004	.066

## R e f e r e n c e s

1. Bogdanova L.N., Dalkarov O.D., Kerbikov B.O., Shapiro I.S. Narrow  $N\bar{N}$  resonances, in Proceedings of the IV International Symposium on nucleon-antinucleon interactions, Editors T.E.Kalogeropoulos, K.C.Wali, Syracuse University, 1975, vol.2, pp. VIII 1-36
2. Kalogeropoulos T.E. The antinucleon-nucleon system at non-relativistic energies, in High-Energy Physics and Nuclear Structure - 1975, AIP, 1975, pp.155-171
3. Shapiro I.S. Interaction of slow antinucleons with nucleons and nuclei. Sov.Phys.Usp., 1973, v.16, p.173  
Bogdanova L.N., Dalkarov O.D., Shapiro I.S. Quasinuclear systems of nucleons and antinucleons. Annals of Physics, 1974, vol.84, No.1-2, pp.261-284
4. Kalogeropoulos T.E., Fillipas T.A., Grammatikakis G. et al. Observation of charge-independence-violating effects in  $\bar{p}d$  annihilations at rest. Phys.Rev.Lett., 1974, v.33, No.27, pp.1631-1635  
Kalogeropoulos T.E., Vayaki A., Grammatikakis G. et al. Observation of excessive and direct  $\gamma$  production in  $\bar{p}d$  annihilations at rest. Phys.Rev.Lett., 1974, v.33, No.27, pp.1635-1637
5. Devons S., Kozlovski T., Nemethy P. et al. Observation of  $\bar{p}p \rightarrow 2\pi^0$  at rest: evidence concerning S-state annihilation. Phys.Rev.Lett., 1971, v.27, No.23, pp.1614-1617
6. Gray L., Papadopoulou Theo, Semipoulou E. et al. Observation on  $\bar{p}d$  annihilation at rest into two pions. Phys. Rev. Lett., 1973, v.30, No.21, pp.1091-1094

7. Bizzarri R., Ciapetti G., Dore U. et al. Comparison of the reaction  $\bar{p}p \rightarrow K^0\bar{K}^0$  at rest in hydrogen and deuterium. A test of S-state annihilation dominance. Nucl. Phys., 1974, v.B69, No.1, pp.307-316
8. Leon M., Bethe H.A. Negative meson absorption in liquid hydrogen. Phys.Rev., 1962, v.127, No.1, pp.636-647
9. Desai B.R. Proton-antiproton annihilation in protonium <sup>(*see*)</sup> Phys.Rev., 1960, v.119, No.4, pp.1385-1389
10. Experiments at CERN in 1975. Experiment P7, CERN-Basel-Karlsruhe-Stockholm Collaboration.
11. Experiments at CERN in 1975. Experiment S142, Daresbury-Mainz-TRIUMF Vancouver Collaboration.
12. Lowenstein D.I. The  $\bar{p}$  and  $\bar{K}$  facilities at BNL AGS, see ref. [1], v.2, pp.VII 1-19
13. Fields T. Antiproton experiment facilities at Argonne, see ref. [1], vol.2, pp.VII 61-67
14. Dover Carl B. Bound states and resonances of the nucleon-antinucleon system, see ref. [1], vol.2, pp.VIII 37-91
15. Snow G.A.  $K^+$  capture process and  $K^-$  nuclear interactions, in Proceedings of the 1960 Annual International Conference on High-Energy Physics at Rochester, Interscience Publishers, New York, 1960, pp.407-414
16. Day T.B., Snow G.A., Sucher J. Suppression of F-state capture in  $(K^-p)$  atoms. Phys.Rev.Lett., 1959, v.3, No.1, pp.61-64
17. Dalkarov O.D., Samoilov V.N. Level shifts and widths of  $\bar{p}p$ -atom. JETP Lett., 1972, v.15, pp.249-251
18. Vermeulen J.L. A solution of the Leon-Bethe model for the Day-Snow-Sucher effect by dynamical group methods. Nucl.Phys., 1969, v.B42, No.3, pp.506-516

19. Russel J.E., Shaw G.L. Collisional de-excitation of ( $\pi^-p$ ) atoms. Phys.Rev.Lett., 1960, v.4, No.7, pp.368-369
20. Kerbikov B.O. On the two-body mesonic-antinucleon annihilation. Phys.Lett., 1973, v.46B, No.2, pp.245-248.



Работа поступила в ОНТИ 3/II-1976г.

---

Подписано к печати 18/II-76г. Т - 03242. Печ. л. 3,0.  
Формат 70 x 108 1/16. Тираж 300 экз. Заказ 25. Цена 16коп.

---

Отдел научно-технической информации ИТЭФ, П17259, Москва